

NOTICE: this is the author's version of a work that was accepted for publication in *Electrochimica Acta*. Changes resulting from the publishing process, such as peer review, editing, corrections, structural formatting, and other quality control mechanisms may not be reflected in this document. Changes may have been made to this work since it was submitted for publication. A definitive version was subsequently published in *Electrochimica Acta*, Vol. 101, (2013). doi: 10.1016/j.electacta.2012.09.104

**Oxygen Reduction Voltammetry on Platinum Macrodisk and Screen-Printed Electrodes in Ionic Liquids: Reaction of the Electrogenerated Superoxide Species with Compounds Used in the Paste of Pt Screen-Printed Electrodes?**

Junqiao Lee,<sup>1</sup> Krishnan Murugappan<sup>1</sup>, Damien W. M. Arrigan<sup>1</sup> and Debbie S. Silvester<sup>1\*</sup>

*Nanochemistry Research Institute, Department of Chemistry, Curtin University, GPOBox U1987, Perth,  
Western Australia 6845*

*Submitted to Electrochimica Acta*

1 ISE member

\*Author to whom all correspondence should be addressed

E.mail: d.silvester-dean@curtin.edu.au

Tel: +61 (0) 892667148

FAX: +61 (0) 892662300

## **Abstract**

Screen-printed electrodes (SPEs) are widely investigated as simple, three-electrode planar surfaces for electrochemical sensing applications, and may be ideal for gas sensing purposes when combined with non-volatile room temperature ionic liquids (RTILs). In this report the suitability of SPEs with RTIL solvents has been investigated for oxygen detection. Oxygen reduction has been studied on commercially available platinum SPEs in eight RTILs. Cyclic voltammetric wave shapes were found to be significantly different on Pt SPE surfaces compared to conventional solid Pt macroelectrodes, suggesting a possible reaction of the electrogenerated superoxide with the compounds that make up the ink/paste of the SPE surface. The only RTIL that did not show such drastically different voltammetry was one that contained a pyrrolidinium cation, suggesting a more chemically stable solvent environment compared to the other imidazolium and phosphonium cations studied. The analytical utility was then studied on four SPE surfaces (carbon, gold, platinum and silver) in two RTILs (one with a pyrrolidinium and one with an imidazolium cation) and linear responses were observed between current and % concentration in the range 10-100 % O<sub>2</sub>. This suggests that SPEs may indeed be suitable for oxygen sensing in some RTILs, but significantly more pre-treatment of the surface is required to obtain reliable results. However, the reaction of superoxide with the SPE ink, together with a noticeable deterioration of the signal over time, suggests that this type of sensing platform may only be suitable for “single-use” oxygen sensing applications.

## **Keywords**

Screen-printed electrodes, oxygen reduction, gas sensing, room temperature ionic liquids, cyclic voltammetry

## 1. Introduction

Screen-printed electrodes (SPEs) are low-cost, disposable sensing surfaces that have been widely used in applications such as glucose biosensing and heavy metal detection since the 1990s. [1,2,3] However, despite their wide use, there is still relatively little fundamental understanding of analyte redox behaviour at these surfaces. Recently, SPEs have become commercialised by a number of companies and are readily available for academic study. As a result, several groups have characterized various commercially available SPEs from companies such as Alderon, Florence, DropSens, Kanichi and Zensor. [4,5,6] In general, it has been reported that SPEs manufactured by DropSens appear to give the best cyclic voltammetric responses (lowest background current, sharpest peak shapes and fastest kinetics). [4,5]

Most SPEs currently reported in the literature are large surface area (e.g. 4 mm diameter) carbon materials, probably due to the low cost of carbon (compared to inert gold and platinum metals). Although manufacturers often do not disclose information on the formulation of the printing inks, they are generally thought to be comprised of synthetic grade graphite or metal particles (the electrochemically active material), vinyl or epoxy-based polymeric binders (to enhance the adhesion properties of the ink to the substrate) and solvents (to improve the viscosity of the ink for the printing process). [4] Carbon-based SPEs usually perform well in aqueous solvents and show similar electrode kinetics to those observed on conventional disk-electrodes. [4,5,6] Gold [7,8] and platinum [9,10] SPEs have also been used, but much more rarely. Moving away from experiments in aqueous-based solvents, we recently found that the background currents of DropSens carbon SPEs are very large compared to Pt and Au SPEs when room temperature ionic liquid (RTIL) solvents are employed. [11] This could be due to the high viscosity and lower “wettability” capabilities of RTILs at carbon surfaces, compared to aqueous solvents. Alternatively, there could be an interaction of the carbon materials with ionic liquids that is causing the screen-printed film to swell or dissolve. This observation should be considered when employing RTILs as solvents in sensing applications using carbon SPEs.

RTILs are liquid solvents (at 298 K) made entirely of ions that possess several properties such as intrinsic conductivity, high thermal stability, high polarity, wide electrochemical windows, low

volatility, high viscosity and good solvating properties. [12,13,14] SPEs in combination with microliter volumes of RTILs are ideal for gas sensing purposes, [15,16] since the RTIL will not evaporate, even under a fast flowing gas stream; microlitre volumes of other solvents (e.g. water or acetonitrile) may only survive for a limited amount of time under such conditions (even at room temperature) and will therefore shorten the lifetime of any sensing device. The additional benefit of using RTILs is that a microliter quantity of the RTIL can be simply drop-cast directly from a bottle of commercially available solvent, with no need for the user to prepare solutions of a solvent containing supporting electrolyte.

Despite the obvious advantages of using RTILs with low-cost SPEs for sensing devices, there has been relatively little work done on fundamental gas behaviour and gas sensing using the RTIL/SPE platform. We recently reported the voltammetry for ammonia oxidation on three SPE surfaces (carbon, platinum and gold) from DropSens. [11] No obvious peaks were observed on carbon SPEs, but it was found that the voltammetry on both Au and Pt SPEs was similar to that observed on Pt microelectrodes in RTILs, suggesting that the electrochemical reaction mechanisms were the same. Stable and reproducible peak currents were observed at different concentrations and a limit of detection of 50 ppm for ammonia on non-modified Pt SPEs was obtained, demonstrating good analytical utility for ammonia sensing. [11] SPEs have also been used for the voltammetric characterization and sensing of oxygen gas [8,17] in RTILs on carbon and gold surfaces. Voltammetric reduction currents for oxygen on carbon SPEs were reported in four common RTILs, showing linear current responses over a concentration range of 20-100 % O<sub>2</sub>. [17] Chemically irreversible voltammetry for O<sub>2</sub> reduction was also reported in three RTILs on Au SPEs, but the analytical utility and reaction mechanism was not investigated. [8]

In this paper, we compare the voltammetric shapes and peak-to-peak separations for the O<sub>2</sub>/O<sub>2</sub><sup>•-</sup> redox couple on a conventional Pt macrodisk electrode in a bulk RTIL volume, to that for Pt SPEs covered with a 7 μL droplet of RTIL. Eight RTILs have been employed, and two RTILs have been chosen for further characterisation on four different SPE surfaces (carbon, gold, platinum and silver). The results obtained reveal the suitability of four types of commercially available SPEs for oxygen gas sensing in RTILs.

## 2. Experimental

### 2.1 Chemical Reagents

The RTILs 1-ethyl-3-methylimidazolium bis(trifluoromethylsulfonyl)imide ( $[\text{C}_2\text{mim}][\text{NTf}_2]$ ), 1-butyl-3-methylimidazolium bis(trifluoromethylsulfonyl)imide ( $[\text{C}_4\text{mim}][\text{NTf}_2]$ ), *N*-butyl-*N*-methylpyrrolidinium bis(trifluoromethylsulfonyl)imide ( $[\text{C}_4\text{mpyrr}][\text{NTf}_2]$ ) and trihexyltetradecylphosphonium bis(trifluoromethylsulfonyl)imide ( $[\text{P}_{14,6,6,6}][\text{NTf}_2]$ ) were synthesized according to standard literature procedures [12,18] and kindly donated by the group of Professor Christopher Hardacre at Queens University, Belfast. The RTILs 1-hexyl-3-methylimidazolium trifluorotris(pentafluoroethyl)phosphate ( $[\text{C}_6\text{mim}][\text{FAP}]$ ), 1-butyl-3-methylimidazolium hexafluorophosphate ( $[\text{C}_4\text{mim}][\text{PF}_6]$ ), 1-butyl-3-methylimidazolium tetrafluoroborate ( $[\text{C}_4\text{mim}][\text{BF}_4]$ ) and trihexyltetradecylphosphonium trifluorotris(pentafluoroethyl)phosphate ( $[\text{P}_{14,6,6,6}][\text{FAP}]$ ), were purchased from Merck KGaA (Kilsyth, Victoria, Australia) at ultra-high purity electrochemical grade (halide content less than 100 ppm). All RTILs were used as received. The chemical structure of the RTILs anions and cations employed in this work are shown in Figure 1. Ethanol (EtOH, Aldrich, 99 %), milli-Q water with a resistance of 18.2  $\text{M}\Omega\cdot\text{cm}$  prepared by a Milli-Q laboratory water purification system (Millipore Pty Ltd., North Ryde, NSW, Australia) and acetonitrile (MeCN, Sigma-Aldrich, 99.8 %) solvents were used for washing the electrodes before and after use with RTILs. High purity oxygen gas (>99.5 %) and high purity nitrogen gas (99.99 %) were purchased from BOC gases (North Ryde, NSW, Australia).

### 2.2 Electrochemical Experiments

All voltammetric experiments were performed using a  $\mu$ -Autolab Type III potentiostat (Eco-Chemie, Netherlands) interfaced to a PC with NOVA 1.8 software, fixing the step potential at 0.003 V. For experiments on the macrodisk electrode, a 1.6 mm diameter platinum electrode (BASi, West Lafayette, Indiana, USA) was polished in a figure-8 motion on soft lapping pads (Buehler, Illinois) prior to each experiment with decreasing particle size of alumina (3  $\mu\text{m}$ , 1  $\mu\text{m}$  and 0.25  $\mu\text{m}$ ). The electrode was sonicated first in water for 15 minutes, and then in ethanol for 15 minutes to remove any alumina particles, followed by washing with acetonitrile and drying under a nitrogen gas stream. The working

electrode was employed in a conventional 3-electrode arrangement, with a 0.5 mm diameter Ag wire reference electrode (Sigma-Aldrich) and a 0.5 mm diameter Pt coil wire counter electrode (Goodfellow Cambridge Ltd., UK) inserted into a home-made glass cell designed to hold up to 3 mL of solvent. The RTIL (~1 mL) was placed in the cell and purged with nitrogen gas for 30 mins (to obtain a blank voltammogram) prior to the introduction of oxygen gas. Oxygen gas (99.5 %) was then bubbled directly into the RTIL with stirring, and cyclic voltammetry was recorded until stable peak currents were observed (typically after ~10 minutes).

For experiments using screen-printed electrodes, a commercially available SPE was inserted into a specially designed glass cell (shown in Figure 2), which is based on the modification of a previously reported T-cell (designed for use with microelectrodes under controlled atmospheres). [19,20] No attempts were made to mechanically polish the electrodes, or to electrochemically “activate” the surfaces using widely-used methods in aqueous solvents [5]. Additionally, the RTILs were not exposed to a vacuum line (commonly employed for experiments using RTILs on micro-disk electrodes) [21] so that the experimental set-up would more closely resemble what is available in a field application for a sensing device. The RTIL (7  $\mu$ L) was drop-cast onto the SPE and spread over the three electrodes, which were connected directly to the potentiostat via soldered wires. The SPE was held in place by insertion through a modified rubber bung so that the working, counter and reference electrodes were inside the cell (with the connections outside) and the electrodes could be placed under a controlled atmosphere of either oxygen, nitrogen or a mixture of these. A glass stopper was inserted into the second tapered joint. The cell was then purged with N<sub>2</sub> gas for more than 30 minutes to remove impurities naturally present in the RTIL (e.g. air, water). When the baseline was stable after pre-conditioning in the RTIL by repeated CV scanning, oxygen gas was introduced into one arm of the cell. The gas was allowed to diffuse into the RTIL until equilibrium was obtained (typically after 15 minutes) and voltammetry was then recorded. Equilibration time was based upon the duration necessary for the stabilization of the open circuit potential monitored on the electrode surface, which may be indicative of the stabilization of the surface conditions of the working electrodes. However, the actual total time required for the equilibration of the gas-concentration in the flow-cell, and the partitioning of the gas-

mixture into the RTIL electrolyte, was found to be much shorter (typically around 4 mins) in separate amperometric experiments. We note here that longer equilibration times were necessary for the partitioning of the gases on SPEs compared to macrodisk experiments despite the much thinner electrolyte layers (i.e. a higher surface area to volume ratios). This has to do with the very small volume of RTIL used on SPEs, which prevents the aggressive bubbling of oxygen gas directly into the RTIL while stirring. Instead, the flowing gas displaces the atmosphere within the flow-cell and the gas is thus slower to partition into the RTIL. Some differences in equilibration times were noticed between the eight studied RTILs, as would be expected given their different viscosities. However, 15 minutes was more than sufficient to achieve equilibrium in all RTILs and was used for consistency in all experiments. Approximately eight repeated CV scans were needed in the presence of 100% O<sub>2</sub> to acquire a stable signal before undertaking measurements. An outlet gas line led from the other arm of the cell into a fume cupboard. All experiments were carried out inside an aluminium Faraday cage to reduce electrical interference, and at a temperature of 293±2 K.

The SPEs were from DropSens (Oviedo, Spain) and consisted of a C, Pt, Au or Ag working electrode surface, Ag quasi-reference electrode and Pt/C counter electrode as detailed in Table 1. The SPEs were purchased from DropSens, since various authors have reported better electrochemical characteristics on DropSens SPEs than on SPEs from other companies. [4,5] Additionally, DropSens SPEs are manufactured on a ceramic substrate that is compatible with RTILs and organic solvents (e.g. acetonitrile), whereas various other commercially available SPEs employ substrates that are only suitable for use in aqueous-based solvents.

### *2.3 Gas-Mixing Set-up*

In order to obtain different concentrations of oxygen, the oxygen line was diluted with nitrogen gas using a gas mixing system (as shown in Figure 2), which consists of two digital flow meters (labelled F1 and F2, from John Morris Scientific, NSW, Australia) connected via a Swagelok T-joint (Swagelok, Kardinya, WA, Australia). The mixed gas then passes through an additional mixing device consisting of two opposing tapered glass needles, inserted into a short piece of PTFE tubing for support



(see enlargement in Figure 2) which increases gas turbulence and ensures adequate mixing of the two gases. The relative flow rates of the flow meters for the two gases, O<sub>2</sub> and N<sub>2</sub>, were used to calculate the % of O<sub>2</sub> introduced into the cell, with the sum of the flow rates kept constant at a total of 250 cm<sup>3</sup>/min. Smaller and larger flow rates were tested in our initial experiments, however the total flow rate of 250 cm<sup>3</sup>/min was chosen as a conservative flow rate such that it was high enough for the gas to quickly displace pre-existing gases within the gas flow cell without depleting the cylinder too quickly. Furthermore, the range, precision and stability of the flow-meters were also taken into account to ensure accurate dilutions could be made using the gas mixing system. Upon switching to a new oxygen concentration, the current response changed within ca. 30 s, but times of up to 10 min after concentration changes were needed to obtain a current that was stable with time in both RTILs studied ([C<sub>2</sub>mim][NTf<sub>2</sub>] and [C<sub>4</sub>mpyrr][NTf<sub>2</sub>]).

#### *2.4 Scanning Electron Microscopy Experiments*

Scanning electron microscopy (SEM) was performed on the working electrode surfaces of the four types of DropSens SPEs employed in this work (carbon, gold, platinum and silver). Images were obtained using a Zeiss Evo 40XVP model, with an accelerating voltage of 10 kV.

### **3. Results and Discussion**

In order to test the suitability of Pt SPEs for oxygen gas sensing in RTILs, cyclic voltammetry for O<sub>2</sub> reduction was recorded on Pt SPEs in eight aprotic RTILs with wide electrochemical windows, namely [C<sub>2</sub>mim][NTf<sub>2</sub>], [C<sub>4</sub>mim][NTf<sub>2</sub>], [C<sub>6</sub>mim][FAP], [C<sub>4</sub>mpyrr][NTf<sub>2</sub>], [C<sub>4</sub>mim][BF<sub>4</sub>], [C<sub>4</sub>mim][PF<sub>6</sub>], [P<sub>14,6,6,6</sub>][NTf<sub>2</sub>] and [P<sub>14,6,6,6</sub>][FAP] (see Figure 1 for ion structures). First, however, it is important to assess the voltammetric responses for oxygen reduction in the eight RTILs on an ideal flat, polished conventional Pt macrodisk electrode, in order for an accurate comparison to be made.

#### *3.1 Oxygen reduction on a Pt macroelectrode in 8 RTILs*

Figure 3 shows typical cyclic voltammetry in eight different RTILs for the reduction of 100 % O<sub>2</sub> (bubbled directly into the RTIL) on a Pt macrodisk electrode (1.6 mm diameter) at a scan rate of 100 mVs<sup>-1</sup>. The blank scans (responses in the absence of oxygen) are shown in Figure 3 as dotted lines. Quasi-reversible voltammetry is observed for O<sub>2</sub> reduction in all eight RTILs, and is believed to due to a simple one-electron reduction mechanism, as commonly reported in aprotic and RTIL solvents: [22,23,24]



Voltammetry for O<sub>2</sub> reduction has been widely reported in the literature in some (but not all) of these RTILs on glassy carbon (GC)/Au/Pt macro-, [22,25,26] Pt/Au/GC micro- [15,23,27,28] and Au micro-array [29] electrodes, with similar voltammetric wave shapes to those observed in Figure 3. Table 2 shows the peak-to-peak separations ( $\Delta E_{pp}$ ) for the O<sub>2</sub>/O<sub>2</sub><sup>•-</sup> redox couple presented in Figure 3. It is obvious that  $\Delta E_{pp}$  varies extensively when the ionic liquid is changed, and is typically in the range 280-520 mV in RTILs containing imidazolium and pyrrolidinium cations. However, a much larger  $\Delta E_{pp}$  is observed in the two tetraalkylphosphonium RTILs, with more than a 1 V separation in [P<sub>14,6,6,6</sub>][NTf<sub>2</sub>] and more than 2 V in [P<sub>14,6,6,6</sub>][FAP]. The unusually wide peak-to-peak separation for O<sub>2</sub>/O<sub>2</sub><sup>•-</sup> has been observed previously on Pt microelectrodes in the same two RTILs with tetraalkylphosphonium cations. [27] Previously, it was suggested that the phosphonium cation acts as a weak acid, giving rise to an ECE reaction. [27] The peak-to-peak separations given in table 2 show no dependence on solvent viscosity, suggesting that other physical properties of the RTIL anions and cations contribute to the different kinetics of the O<sub>2</sub>/O<sub>2</sub><sup>•-</sup> redox couple. Generally, the data presented in Figure 3 and table 2 corresponds well to that reported at conventional solid electrodes and can act as a comparison to the voltammetry that is observed on SPEs in the next section.

### 3.2 Oxygen reduction on Pt screen-printed electrodes in 8 RTILs

Figure 4 shows typical cyclic voltammetry in eight different RTILs for the reduction of 100 % O<sub>2</sub> (flowed directly over a microlitre droplet of RTIL) on a Pt SPE (4.0 mm diameter) at a scan rate of 100 mVs<sup>-1</sup>. Both the first (dot dashed line) and second (solid line) voltammetric scans are presented, along

with the response in the absence of oxygen (dotted line). It was observed that the first scans were generally substantially different (with respect to shape, peak potential and peak current). However, the second and subsequent scans were generally similar, but up to eight repeat scans in the presence of O<sub>2</sub> were necessary for the peak currents and positions observed to fully stabilize. It is clearly evident from this figure that the voltammetric wave shapes are drastically different on the SPEs compared to the macrodisk electrode (Figure 3). In particular, in five of the RTILs tested, a significant closeness or “cross-over” between the cathodic and anodic scans was observed in the voltammetry. This suggests that the surface has somehow been modified or changed as a result of the oxygen reduction reaction. The lack of an anodic reverse peak in these five RTILs also indicates that there is a follow-up chemical reaction occurring, removing the electrogenerated superoxide from the surface. We suggest that the cause of the cross-over voltammetry may be due to a chemical reaction of the superoxide with one or more of the compounds present in the paste of the SPE’s working electrode. In order to test this theory, small amounts of particles from a Pt SPE were scraped into a vial, sonicated in 10 μL of acetonitrile, and drop-cast onto a Pt macrodisk electrode. The modified electrode was then placed in one of the RTILs where cross-over voltammetry was observed ([C<sub>2</sub>mim][NTf<sub>2</sub>]) and oxygen voltammetry was recorded. The resulting voltammogram (presented as a thick line in Figure 5) shows cross-over voltammetry very similar to that reported in Figure 4a, but which was absent from the voltammetry at an un-modified Pt macrodisk electrode (thin line in Figure 5). This rules out the possibility that the altered voltammetry is caused by other factors (e.g. reactions with the ceramic substrate, reference electrode or counter electrode, or impurities in the RTIL). We note here that chemically irreversible voltammetry for oxygen reduction on *gold* screen-printed electrodes in three imidazolium ionic liquids has also been reported by Gebicki et al., [8] but the cause of the irreversible voltammetry was unknown. It is highly possible that a similar reaction also occurs with superoxide and ink/pastes in the Au SPEs (and this will be discussed later in section 3.3.3). It should be noted that in our previous work on ammonia gas oxidation on C, Pt and Au SPEs in [C<sub>2</sub>mim][NTf<sub>2</sub>], [11] no unusual voltammetry or change in reaction mechanism was observed on SPEs (compared to conventional solid electrodes), suggesting that the

reaction with particles in the pastes of SPEs only occurs when highly reactive species such as superoxide are present.

Another possible explanation for the unusual voltammetry is that the products from the SPE counter electrode are reaching the working electrode on the timescale of the experiment. Using the equation:

$$t = \frac{d^2}{D} \quad (2)$$

where  $t$ =time,  $d$ =distance and  $D$ =diffusion coefficient, taking a time of 50 seconds (two consecutive voltammograms over 5 V at 100 mVs<sup>-1</sup>) and using a generous value for  $D$  of  $10 \times 10^{-10}$  m<sup>2</sup>s<sup>-1</sup>, the products of the counter electrode process could travel ca. 0.22 mm. Since the working and counter electrode are separated by 1 mm, this implies that the closely-positioned working and counter electrode are not likely to cross-contaminate each other in the ionic liquid (although this may be a possibility in an aqueous sample).

Also in Figure 4, there is no well-defined O<sub>2</sub> reduction peak on the SPE surface in the two RTILs that contain the [P<sub>14,6,6,6</sub>]<sup>+</sup> cation, only a gradual increase in reduction current until the edge of the available electrochemical window. This suggests that these two RTILs are not suitable for oxygen sensing on Pt SPEs. Interestingly, in one out of the eight RTILs studied ([C<sub>4</sub>mpyrr][NTf<sub>2</sub>], Figure 4d), the shape of the voltammetry on SPEs is relatively similar to that on a conventional macrodisk electrode. The clear existence of an oxidation peak on the reverse sweep in Figure 4d indicates that the electrogenerated superoxide is stable and re-oxidised back to oxygen at ~-0.9 V vs Ag. The peak-to-peak separation for the O<sub>2</sub>/O<sub>2</sub><sup>•-</sup> redox couple in [C<sub>4</sub>mpyrr][NTf<sub>2</sub>] on Pt SPEs (355 mV) is only slightly larger than on the Pt macroelectrode (331 mV), suggesting that the two surfaces give rise to similar kinetics. It is unclear why the reaction is chemically reversible in only this particular RTIL, but it may be due to the more chemically and electrochemically inert pyrrolidinium cation (as demonstrated by Compton and Wibowo who showed only this RTIL and two other tetraalkylammonium RTILs were capable of supporting alkali metal deposition. [REF]). In the literature, it has been suggested that both imidazolium and phosphonium cations are weakly acidic [12,27] and may partake in an acid-base reaction in the presence of highly basic species (e.g. superoxide). Although this acid-base reaction is not

observed for O<sub>2</sub> reduction on conventional solid electrodes (e.g. Figure 3), it appears that the combination of superoxide with compounds in the pastes of SPEs may give rise to very basic species that may then react with the weakly acidic RTIL cations. However, the pyrrolidinium cation ([C<sub>4</sub>mpyrr]<sup>+</sup>) does not have an acidic proton and may offer a stabilizing effect of the superoxide at the screen-printed surface, preventing the chemical reaction that occurs on SPEs in the other RTILs.

Experiments were also conducted on mixtures of [C<sub>4</sub>mpyrr][NTf<sub>2</sub>] and [C<sub>2</sub>mim][NTf<sub>2</sub>] RTILs, in order to determine at what volume ratio of the mixture the reaction becomes chemically reversible on Pt SPEs, and the results are presented in Figure 6 (on the same axes scales). A larger reduction peak current is observed in [C<sub>2</sub>mim][NTf<sub>2</sub>] (Figure 6d) compared to [C<sub>4</sub>mpyrr][NTf<sub>2</sub>] (Figure 6a), likely due to the different solvent viscosities and the amount of partitioning of oxygen into the RTIL. The voltammetry of the mixtures (presented in figure 6b and 6c) reveals that crossover is sensitive to the composition of the RTIL medium. At volume ratios of 50:50 [C<sub>4</sub>mpyrr][NTf<sub>2</sub>]:[C<sub>2</sub>mim][NTf<sub>2</sub>], the voltammetry exhibits this crossover characteristic, however when 60% or more of [C<sub>4</sub>mpyrr][NTf<sub>2</sub>] is present, the crossover is not present. Additionally, the relative height of the superoxide oxidation peak increases with increasing ratio of [C<sub>4</sub>mpyrr][NTf<sub>2</sub>] in the mixture. This is an extremely interesting observation and highlights that the choice of RTIL is very important for electrochemical reactions where highly reactive species are present.

### *3.3 Oxygen reduction on four different SPE surfaces in RTILs*

Since we have shown that the voltammetry for O<sub>2</sub> reduction on a Pt SPE is significantly different to that on a macrodisk electrode in seven of the eight RTILs, it is useful to also study other screen-printed working electrode surfaces to see if similar behaviour occurs, and ultimately to see if this affects the analytical utility of the surface for oxygen sensing. Four common working electrode surfaces (carbon, gold, platinum and silver) were employed for this study, and cyclic voltammograms have been recorded at various concentrations of O<sub>2</sub>. Two RTILs have been chosen for this study; one where no obvious cross-over voltammetry is observed on SPEs ([C<sub>4</sub>mpyrr][NTf<sub>2</sub>]) and one where obvious cross-over

occurs ( $[C_2mim][NTf_2]$ ). It is also useful to look at the structure of the DropSens SPE surfaces using imaging techniques to see if this can be related to the observed voltammetry.

### 3.3.1 Surface structure of four different screen-printed working electrodes

Scanning electron microscopy (SEM) images of the four DropSens working electrode surfaces were recorded to investigate and compare their topography and structure. Figure 7 shows the SEM images obtained for C, Au, Pt and Ag SPE surfaces. The images show that the carbon surface has flake-like particles and cracks indicating that the particles are not held together strongly. On the gold surface tiny particles that correspond to crystalline gold are present. It can also be seen that the platinum surface is more porous compared to silver and gold surfaces, and the general appearance of the silver SPE is smoother than the other three surfaces. It is clear from these images that the porosity and roughness of the SPE surfaces are significantly different depending on the material used for the working electrode, and this in turn may affect the voltammetry.

### 3.3.2 Analytical utility for oxygen reduction on four different SPEs in $[C_4mpyrr][NTf_2]$

Figure 8 shows the reduction of oxygen at different concentrations (0, 10, 20, 40, 60, 80 and 100 % by volume, nitrogen fill) in the RTIL  $[C_4mpyrr][NTf_2]$  on four SPE surfaces (C, Au, Pt and Ag). The measurements were performed when the voltammetry had stabilized after initial reductive scans. On all surfaces, chemically reversible reduction waves are seen and the peak currents increase with increasing  $O_2$  concentration (as previously reported on Au microelectrodes, [23] Pt macroelectrodes [25] and carbon SPEs [17] in RTILs). On the carbon SPE (Figure 8a), a very high background current is observed in RTILs (as we previously reported when studying ammonia oxidation on SPEs). [11] There are also some small impurity peaks present (e.g. oxidation peak at  $\sim -0.5$  V on C,  $\sim -1.0$  V on Au, and reduction peak at  $\sim -0.8$  V on Ag), which are also present in the blank scans (dotted lines). Contributing factors to these peaks may include the fact that the surfaces were not polished or cleaned before experiments, the presence of intrinsic electrochemically active materials in the SPE pastes, and the fact that the RTIL was not evacuated prior to experiments (see experimental section for more details). However, these peaks do

not interfere with the measurements of peak currents due to oxygen reduction since background subtraction was employed.

The relative magnitude of the peak current varies between the carbon, gold and platinum surfaces, despite the screen-printed working-electrode surfaces reportedly having the same diameter (4.0 mm, as reported in Table 1). Assuming that the transport of oxygen to the electrode is fully diffusion controlled, this suggests that the electrochemically active area varies between the three surfaces, and is unsurprising considering the different surface structures observed in the SEM images (Figure 7). In Figure 8, the reduction peak on carbon is roughly twice as large as on Au, while the peak on Pt is approximately two thirds that of Au. The diameter of the silver surface is significantly smaller (1.6 mm) than C, Au and Pt, and as a result, the current on Ag is approximately  $1/7^{\text{th}}$  compared to Au.

A very important observation to note is that after experiments using C SPEs for O<sub>2</sub> sensing, the RTIL solvent became brownish black, probably due to materials from the C SPE leaching from the electrode surface into the RTIL. This is supported by the observation that after removing the RTIL from the surface, the surface looked faded in comparison to a fresh C SPE. This was only found to happen when a potential is applied and does not occur when the surface is simply covered with the RTIL for extended periods of time. However, despite the obvious degradation of the carbon surface, cyclic voltammetry can still be recorded at different concentrations and reasonable calibration graphs could be extracted.

The insets to Figure 8 show the corresponding plots of (baseline corrected) peak current versus % O<sub>2</sub> and the best-fit straight-line. The equations for the calibration curves and their linear regression coefficient ( $R^2$ ) values are given in the top half of Table 3. The calculated limits of detection (LOD) were based on three times the standard deviation of the intercept and are within the low percentage range (4-20 %). For a real oxygen sensor, the ability to measure between ~5-20 % O<sub>2</sub> in the atmosphere is sufficient, since in most real-world conditions, the concentration of O<sub>2</sub> lies near 20 %. Anything less than this requires investigation, so a sensor with a linear response from a few % up to 20 % concentrations is optimal. All SPEs satisfy this requirement, with the exception of carbon, possibly due to the degradation of the surface during potential cycling in RTILs (discussed earlier). In spite of the

excellent  $R^2$  values reported in Table 3, the voltammetry was observed to vary between experiments and was dependent on the pre-conditioning steps taken, as highlighted in the experimental section. We also note that the voltammetry can shift on the potential axis, probably due to the unstable silver quasi-reference electrode. For the monitoring of oxygen using these types of sensors with  $[C_4\text{mpyrr}][\text{NTf}_2]$ , it was found that the calibration curves for separate fresh screen-printed electrodes used straight out of the box were almost identical initially, and calibration does not need to be performed on every electrode. However, after one set of experiments on the same screen-printed electrode, the calibration curves tend to deviate from one another and require re-calibrating before continued experiments.

### *3.3.3 Analytical utility for oxygen reduction on four different SPEs in $[C_2\text{mim}][\text{NTf}_2]$*

Since significant cross-over of the voltammetry was observed on Pt surfaces  $[C_2\text{mim}][\text{NTf}_2]$  (Figure 4a), it is of interest to see if this occurs at other surfaces in this RTIL, and ultimately if this affects the sensing ability of the surface. Figure 9 shows the reduction of oxygen at different concentrations (0, 10, 20, 40, 60, 80 and 100 %) in  $[C_2\text{mim}][\text{NTf}_2]$  on four SPEs (C, Au, Pt and Ag). The measurements were performed when the voltammetry had stabilized after initial reductive scans. On carbon, there is again a large background charging current, but the reduction peak for  $O_2$  can be clearly distinguished at different concentrations. However, there is no obvious superoxide oxidation peak, suggesting that the product may have reacted with compounds in the C SPE paste in this RTIL. It can be seen from Figure 9 that the cathodic and anodic scans on Au and Ag surfaces also are very close together, although this effect is not as dramatic as on Pt surfaces, where the scans crossed over. There is a much smaller superoxide oxidation peak on Au and Ag in  $[C_2\text{mim}][\text{NTf}_2]$  compared to  $[C_4\text{mpyrr}][\text{NTf}_2]$ , suggesting that the Au and Ag surfaces may also have been changed/modified as the result of reaction products of the superoxide/paste/RTIL interaction. There are also additional oxidation peaks between -0.5 and 0 V on all four surfaces, which may be oxidations of these reduction products at the SPEs. However, despite the unusual wave shapes on the four surfaces, the reduction peak currents are seen to increase linearly with concentration of  $O_2$ , as shown in the insets to Figure 9. The equations for the best-fit straight-lines are given in the bottom half of Table 3, together with their  $R^2$  value. Excellent linearity is observed with



$R^2 > 0.99$  on all four SPEs, and C, Au and Pt were very similar with regards to sensitivity ( $\sim 1 \mu\text{A} [\% \text{O}_2]^{-1}$ ). Similar limits of detection (few %) were obtained in this RTIL as in  $[\text{C}_4\text{mpyrr}][\text{NTf}_2]$ , however more pre-conditioning scans were found to be necessary before the voltammetry stabilizes. Additionally, the signals were found to degrade more quickly over prolonged use in this RTIL, possibly due to a build-up of the reaction product from the superoxide/SPE paste/RTIL reaction. In both RTILs, the silver surface gave rise to the most reproducible voltammetry and was also the easiest surface in which to regain a reliable blank signal (under a nitrogen atmosphere) after experiments. It was impossible to regain a featureless blank signal on the other three surfaces after the calibration experiments had been performed in this RTIL, suggesting that long-term monitoring of oxygen may not be possible on C, Au and Pt SPEs in this RTIL.

#### 4. Conclusions

Cyclic voltammetry for oxygen reduction in eight RTILs has been presented on Pt macrodisk electrodes and Pt SPEs, with significantly different voltammetric wave shapes observed on the two types of surface. An obvious cross-over of the voltammetry on SPEs indicates that the surface has been modified, possibly as a result of a reaction of the electrogenerated superoxide with compounds in the Pt SPE ink/paste. The only RTIL that did not show this effect was [C<sub>4</sub>mpyrr][NTf<sub>2</sub>], suggesting there may be a stabilizing effect from the less acidic and more chemically stable pyrrolidinium cation (compared to imidazolium and phosphonium). Despite the obvious change in voltammetry and reaction mechanism, plots of peak current vs % concentration O<sub>2</sub> were linear in both [C<sub>4</sub>mpyrr][NTf<sub>2</sub>] and [C<sub>2</sub>mim][NTf<sub>2</sub>], suggesting that SPEs with RTILs may indeed be viable sensing surfaces for oxygen (with silver being the best surface in terms of reproducibility). However, significantly more pre-treatment of the SPE surface is required (compared to solid micro- or macro- electrodes) before reproducible measurements can be made. Additionally, the signal degenerates much more rapidly on SPEs (particularly in RTILs where the cross-over was seen), suggesting that these types of commercially available SPEs may only be a “single-use” sensing surface for oxygen detection in RTILs.

#### Acknowledgements

The authors thank Professor Christopher Hardacre at Queens University Belfast for the kind donation of four of the ionic liquids used in this work. DSS thanks Curtin University for funding via a Curtin Research Fellowship and the Australian Research Council for a Discovery Early Career Researcher Award (DECRA: DE120101456). JL and KM thank Curtin University for the award of Curtin International Postgraduate Research Scholarships. The authors also acknowledge the use of equipment, scientific and technical assistance of the Curtin University Electron Microscope Facility, which is partially funded by the University, State and Commonwealth Governments of Australia.

## References:

- [1] U. Bilitewski, G.C. Chemnitz, P. Riiger, R.D. Schmid, *Sens. Act. B* 7 (1992) 351.
- [2] J.P. Hart, S.A. Wering, *Trends Anal. Chem.* 16 (2) (1997) 89.
- [3] R. Nagata, S.A. Clark, K. Yokoyama, E. Tamiya, I. Karube, *Anal. Chim. Acta* 304 (1995) 157.
- [4] P. Fanjul-Bolado, D. Hernández-Santos, P.J. Lamas-Ardisana, A. Martín-Pernía, A. Costa-García, *Electrochim. Acta* 53 (2008) 3635.
- [5] R.O. Kadara, N. Jenkinson, C.E. Banks, *Sens. Act. B* 138 (2009) 556.
- [6] J. Prasek, L. Trnkova, I. Gablech, P. Businova, J. Drbohlavova, J. Chomoucka, V. Adam, R. Kizek, J. Hubalek, *Int. J. Electrochem. Sci.* 7 (2012) 1785.
- [7] R. García-González, M.T. Fernández-Abedul, A. Pernía, A. Costa-García, *Electrochim. Acta* 53 (2008) 3242.
- [8] J. Gebicki, A. Kloskowski, W. Chrzanowski, *Electrochim. Acta* 56 (2011) 9910.
- [9] C.-H. Chou, J.-L. Chang, J.-M. Zen, *Electroanalysis* 21 (2) (2009) 206.
- [10] J.P. Metters, F. Tan, R.O. Kadara, C.E. Banks, *Anal. Methods* 4 (2012) 1272.
- [11] K. Murugappan, J. Lee, D.S. Silvester, *Electrochem. Commun.* 13 (2011) 1435.
- [12] P.A.D. Bonhôte, N. Papageorgiou, K. Kalyanasundaram, M. Grätzel, *Inorg. Chem.* 35 (1996) 1168.
- [13] M.C. Buzzeo, R.G. Evans, R.G. Compton, *ChemPhysChem* 5 (2004) 1106.
- [14] D.S. Silvester, R.G. Compton, *Z. Phys. Chem.* 220 (2006) 1247.
- [15] M.C. Buzzeo, C. Hardacre, R.G. Compton, *Anal. Chem.* 76 (2004) 4583.
- [16] D.S. Silvester, *Analyst* 136 (2011) 4871.
- [17] S.-Q. Xiong, Y. Wei, Z. Guo, X. Chen, J. Wang, J.-H. Liu, X.-J. Huang, *J. Phys. Chem. C* 115 (35) (2011) 17471.
- [18] D.R. MacFarlane, P. Meakin, J. Sun, N. Amini, *J. Phys. Chem. B* 103 (1999) 4164.
- [19] U. Schröder, J.D. Wadhawan, R.G. Compton, F. Marken, P.A.Z. Suarez, C.S. Consorti, R.F. de Souza, J. Dupont, *New J. Chem.* 24 (2000) 1009.
- [20] D.S. Silvester, A.J. Wain, L. Aldous, C. Hardacre, R.G. Compton, *J. Electroanal. Chem.* 596 (2006) 131.
- [21] L.E. Barrosse-Antle, A.M. Bond, R.G. Compton, A.M. O'Mahony, E.I. Rogers, D.S. Silvester, *Chem. Asian J.* 5 (2010) 202.
- [22] I.M. AlNashef, M.L. Leonard, M.C. Kittle, M.A. Matthews, J.W. Weidner, *Electrochem. Solid-State Lett.* 4 (2001) D16.
- [23] M.C. Buzzeo, O.V. Klymenko, J.D. Wadhawan, C. Hardacre, K.R. Seddon, R.G. Compton, *J. Phys. Chem. A* 107 (2003) 8872.
- [24] D.T. Sawyer, G. Chiericato, Jr., C.T. Angelis, E.J. Nanni, Jr., T. Tsuchiya, *Anal. Chem.* 54 (1982) 1720.
- [25] R. Toniolo, N. Dossi, A. Pizzariello, A.P. Doherty, S. Susmel, G. Bontempelli, *J. Electroanal. Chem.* 670 (2012) 23.
- [26] Z. Wang, P. Lin, G.A. Baker, J. Stetter, X. Zeng, *Anal. Chem.* 83 (2011) 7066.
- [27] R.G. Evans, O.V. Klymenko, S.A. Saddoughi, C. Hardacre, R.G. Compton, *J. Phys. Chem. B* 107 (2004) 7878.
- [28] X.-J. Huang, E.I. Rogers, C. Hardacre, R.G. Compton, *J. Phys. Chem. B* 113 (2009) 8953.
- [29] X.-J. Huang, L. Aldous, A.O. O'Mahony, F.J. del Campo, R.G. Compton, *Anal. Chem.* 82 (2010) 5238.

## Tables

**Table 1.** Technical parameters including the nature of working, counter and reference electrodes employed in the SPEs used in this study (according to the DropSens Co. database)

Supplier	Code	WE material	WE diameter	CE material	RE material
DropSens	DRP-110	Carbon	4 mm	Carbon	Silver
DropSens	DRP-250AT	Gold	4 mm	Platinum	Silver
DropSens	DRP-550	Platinum	4 mm	Platinum	Silver
DropSens	DRP-C013	Silver	1.6 mm	Carbon	Silver

**Table 2.** Peak-to-peak separations for the  $O_2/O_2^{\cdot-}$  redox couple obtained on a Pt macrodisk electrode (Figure 3) and on a Pt SPE (Figure 4) in eight RTILs, in order of increasing solvent viscosity.

RTIL	Viscosity at 298 K/ cP [21]	$\Delta E_{pp}(O_2/O_2^{\cdot-})$ on Pt macrodisk / mV	$\Delta E_{pp}(O_2/O_2^{\cdot-})$ on Pt SPE / mV
[C <sub>2</sub> mim][NTf <sub>2</sub> ]	34	314	-
[C <sub>4</sub> mim][NTf <sub>2</sub> ]	52	462	-
[C <sub>6</sub> mim][FAP]	74	518	-
[C <sub>4</sub> mpyrr][NTf <sub>2</sub> ]	89	331	355
[C <sub>4</sub> mim][BF <sub>4</sub> ]	112	269	-
[C <sub>4</sub> mim][PF <sub>6</sub> ]	371	278	-
[P <sub>14,6,6,6</sub> ][NTf <sub>2</sub> ]	450	1051	No reduction peak
[P <sub>14,6,6,6</sub> ][FAP]	464	2197	No reduction peak

**Table 3.** Equations for the best-fit straight line for the calibration graphs presented in Figures 8 and 9, and corresponding limits of detection (LOD) based on 3 standard deviations from the blank.

RTIL	SPE surface	Equation of calibration graph	R <sup>2</sup>	LOD / %
[C <sub>4</sub> mpyrr][NTf <sub>2</sub> ]	C	$-i = 1.07 \times 10^{-6} [O_2] + 4.54 \times 10^{-5}$	0.985	20.7
	Au	$-i = 7.13 \times 10^{-7} [O_2] + 1.58 \times 10^{-6}$	0.999	4.5
	Pt	$-i = 6.40 \times 10^{-7} [O_2] + 4.02 \times 10^{-6}$	0.998	7.9
	Ag	$-i = 1.56 \times 10^{-7} [O_2] + 7.94 \times 10^{-7}$	0.998	6.4
[C <sub>2</sub> mim][NTf <sub>2</sub> ]	C	$-i = 1.93 \times 10^{-6} [O_2] + 2.71 \times 10^{-6}$	0.999	1.5
	Au	$-i = 1.79 \times 10^{-6} [O_2] + 1.38 \times 10^{-6}$	0.999	4.0
	Pt	$-i = 1.88 \times 10^{-6} [O_2] - 5.93 \times 10^{-6}$	0.999	3.3
	Ag	$-i = 4.20 \times 10^{-7} [O_2] + 2.45 \times 10^{-6}$	0.997	8.9

## Figure Legends

**Figure 1.** Chemical structures and nomenclature for the RTIL anions and cations employed in this work

**Figure 2.** Schematic of the gas mixing system and glass cell used for voltammetric measurements on screen-printed electrodes. F1 and F2 are digital flow meters.

**Figure 3.** Cyclic voltammograms on a conventional platinum macrodisk electrode (diameter 1.6 mm) at a scan rate  $100 \text{ mVs}^{-1}$  for the reduction of 100 %  $\text{O}_2$  in eight RTILs: (a)  $[\text{C}_2\text{mim}][\text{NTf}_2]$ , (b)  $[\text{C}_4\text{mim}][\text{NTf}_2]$ , (c)  $[\text{C}_6\text{mim}][\text{FAP}]$ , (d)  $[\text{C}_4\text{mpyrr}][\text{NTf}_2]$ , (e)  $[\text{C}_4\text{mim}][\text{BF}_4]$ , (f)  $[\text{C}_4\text{mim}][\text{PF}_6]$ , (g)  $[\text{P}_{14,6,6,6}][\text{NTf}_2]$  and (h)  $[\text{P}_{14,6,6,6}][\text{FAP}]$ . The dotted line is the response in the absence of oxygen.

**Figure 4.** Cyclic voltammograms on a screen-printed DropSens platinum electrode (diameter 4.0 mm) at a scan rate  $100 \text{ mVs}^{-1}$  for the reduction of 100 %  $\text{O}_2$  in eight RTILs: (a)  $[\text{C}_2\text{mim}][\text{NTf}_2]$ , (b)  $[\text{C}_4\text{mim}][\text{NTf}_2]$ , (c)  $[\text{C}_6\text{mim}][\text{FAP}]$ , (d)  $[\text{C}_4\text{mpyrr}][\text{NTf}_2]$ , (e)  $[\text{C}_4\text{mim}][\text{BF}_4]$ , (f)  $[\text{C}_4\text{mim}][\text{PF}_6]$ , (g)  $[\text{P}_{14,6,6,6}][\text{NTf}_2]$  and (h)  $[\text{P}_{14,6,6,6}][\text{FAP}]$ . Dot dashed line is the first scan, solid line is the second scan and dotted line is the response in the absence of oxygen.

**Figure 5.** Cyclic voltammetry for 100 %  $\text{O}_2$  in  $[\text{C}_2\text{mim}][\text{NTf}_2]$  at a scan rate of  $100 \text{ mVs}^{-1}$ . Thin line=response on a bare Pt macrodisk electrode ( $d=1.6 \text{ mm}$ ) and thicker line= response on the same electrode covered with Pt SPE particles.

**Figure 6.** Cyclic voltammetry for 100 %  $\text{O}_2$  on a DropSens Pt electrode at a scan rate of  $100 \text{ mVs}^{-1}$  in electrolytes with different  $[\text{C}_4\text{mpyrrNTf}_2]:[\text{C}_2\text{mimNTf}_2]$  mixing-ratios. (a) 100:0, (b) 60:40, (c) 50:50 and (d) 0:100.

**Figure 7.** Scanning electron micrographs of untreated DropSens working electrodes. (a) Carbon, (b) gold, (c) platinum and (d) silver screen-printed electrodes

**Figure 8.** Cyclic voltammetry for  $\text{O}_2$  reduction in  $[\text{C}_4\text{mpyrr}][\text{NTf}_2]$  on (a) C, (b) Au, (c) Pt and (d) Ag SPEs at 10, 20, 40, 60, 80 and 100 vol %  $\text{O}_2$  at a scan rate of  $100 \text{ mVs}^{-1}$ . The dotted line is the response in the absence of oxygen. The insets are the corresponding plots of reduction peak current vs vol %  $\text{O}_2$  and the line of best-fit.

**Figure 9.** Cyclic voltammetry for  $\text{O}_2$  reduction in  $[\text{C}_2\text{mim}][\text{NTf}_2]$  on (a) C, (b) Au, (c) Pt and (d) Ag SPEs at 10, 20, 40, 60, 80 and 100 vol %  $\text{O}_2$  at a scan rate of  $100 \text{ mVs}^{-1}$ . The dotted line is the response

in the absence of oxygen. The insets are the corresponding plots of reduction peak current vs vol % O<sub>2</sub> and the line of best-fit.

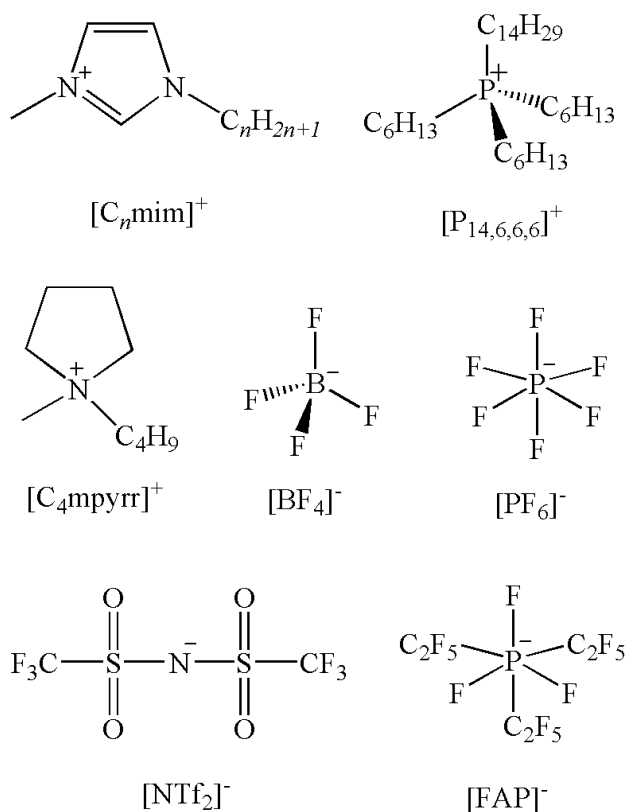


**Figure 1.** Chemical structures and nomenclature for the RTIL anions and cations employed in this work

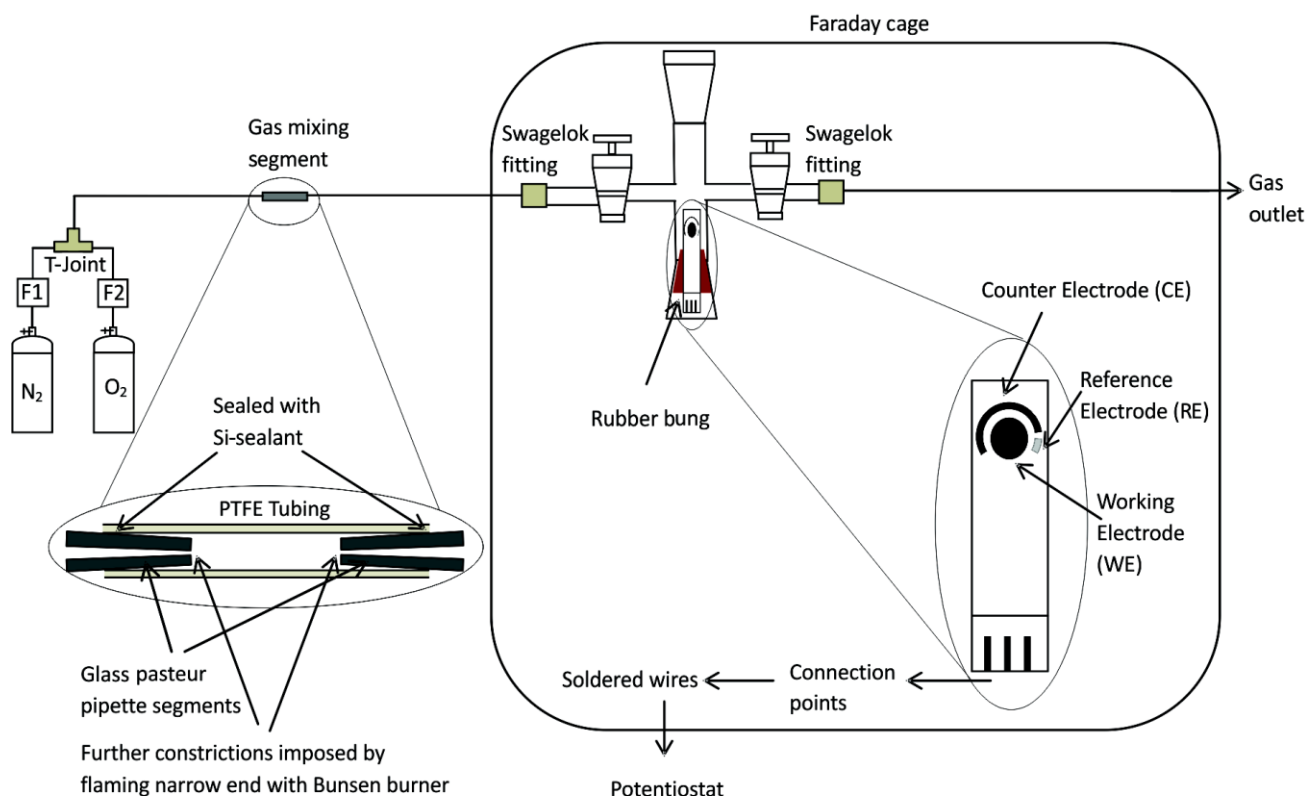


**Figure 2.** Schematic of the gas mixing system and glass cell used for voltammetric measurements on screen-printed electrodes. F1 and F2 are digital flow meters.

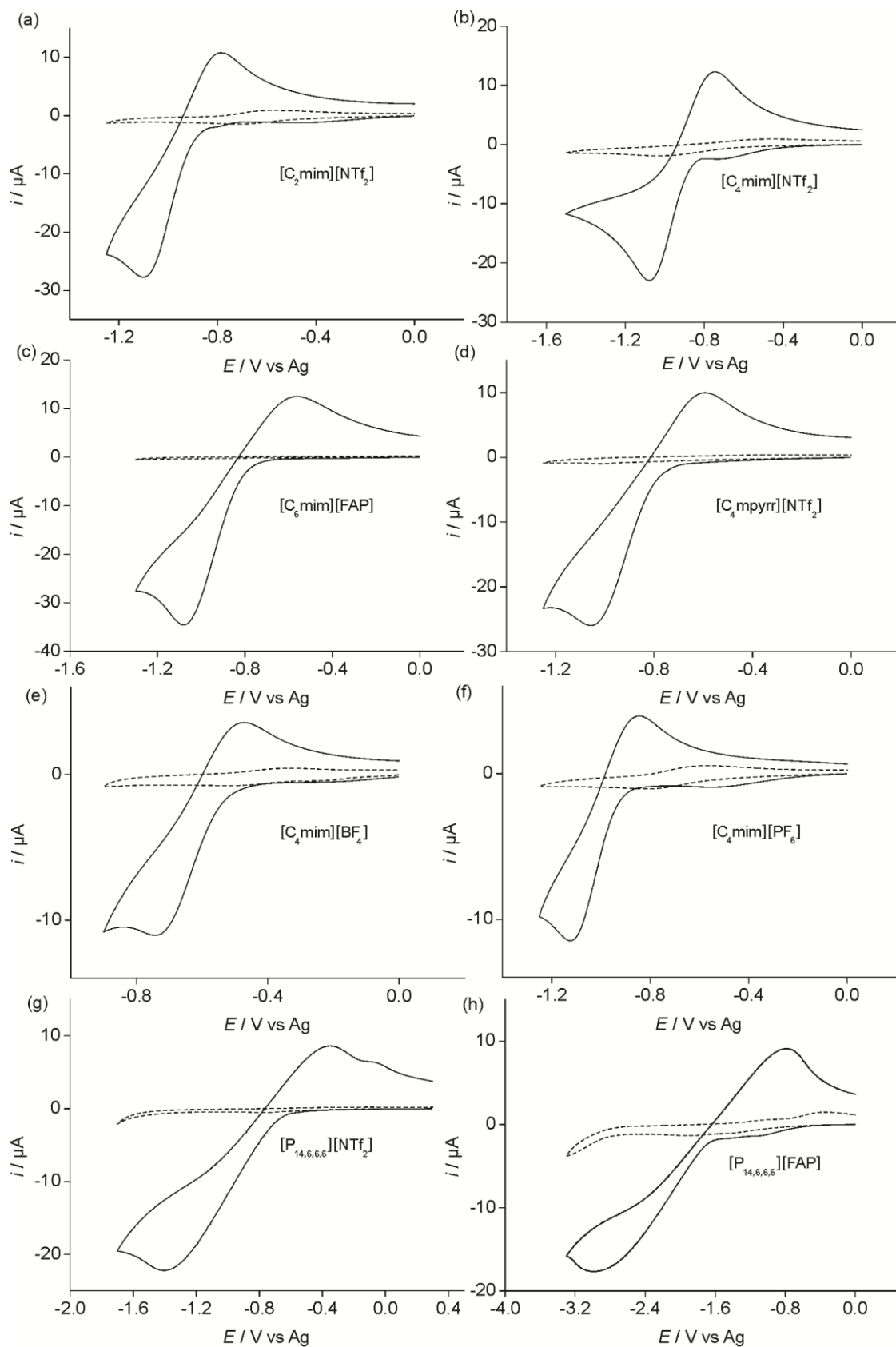


**Figure 3.** Cyclic voltammograms on a conventional platinum macrodisk electrode (diameter 1.6 mm) at a scan rate  $100 \text{ mVs}^{-1}$  for the reduction of 100 %  $\text{O}_2$  in eight RTILs: (a)  $[\text{C}_2\text{mim}][\text{NTf}_2]$ , (b)  $[\text{C}_4\text{mim}][\text{NTf}_2]$ , (c)  $[\text{C}_6\text{mim}][\text{FAP}]$ , (d)  $[\text{C}_4\text{mpyrr}][\text{NTf}_2]$ , (e)  $[\text{C}_4\text{mim}][\text{BF}_4]$ , (f)  $[\text{C}_4\text{mim}][\text{PF}_6]$ , (g)  $[\text{P}_{14,6,6,6}][\text{NTf}_2]$  and (h)  $[\text{P}_{14,6,6,6}][\text{FAP}]$ . The dotted line is the response in the absence of oxygen.



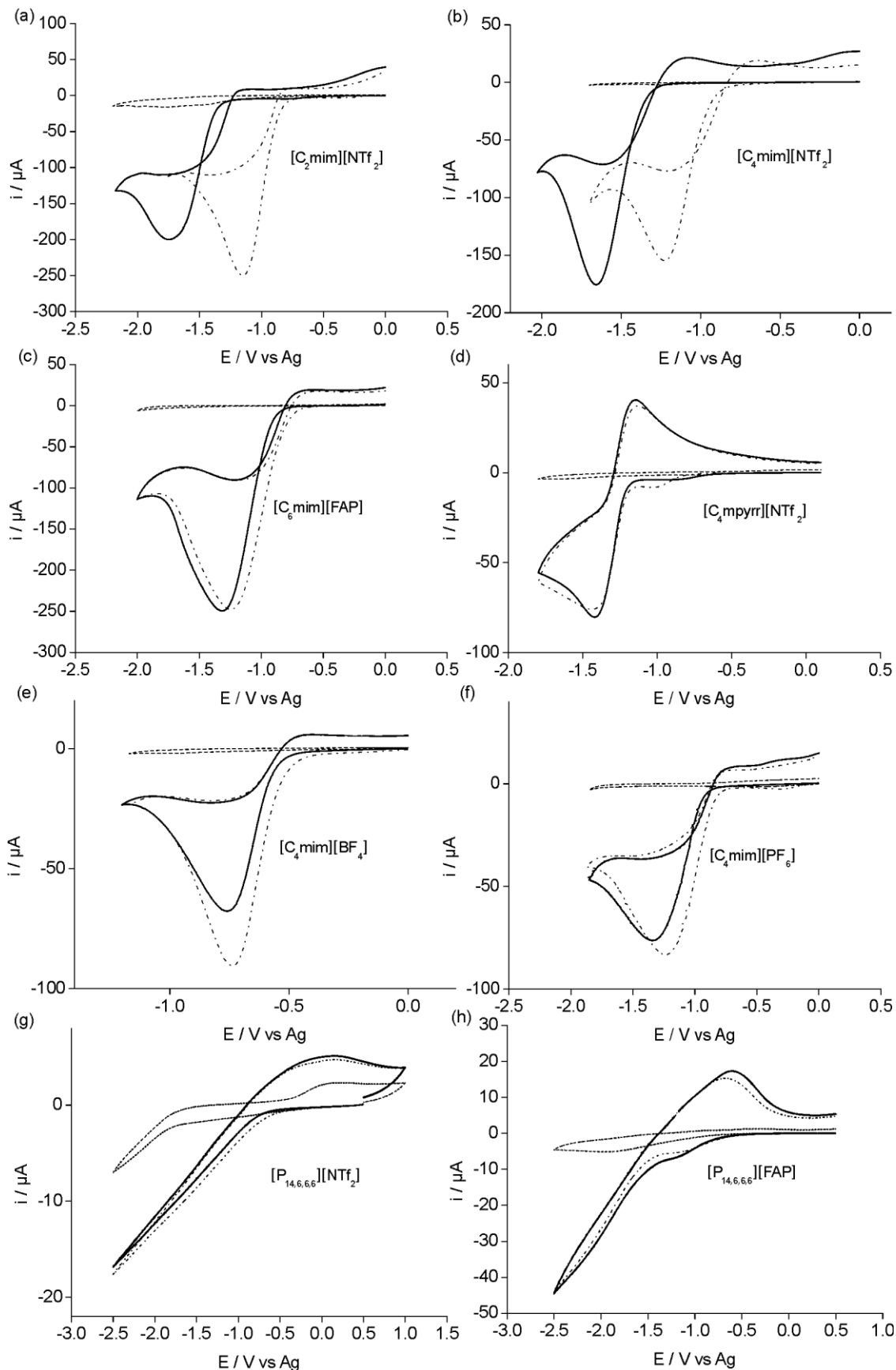


**Figure 4.** Cyclic voltammograms on a screen-printed DropSens platinum electrode (diameter 4.0 mm) at a scan rate  $100 \text{ mVs}^{-1}$  for the reduction of 100 %  $\text{O}_2$  in eight RTILs: (a)  $[\text{C}_2\text{mim}][\text{NTf}_2]$ , (b)  $[\text{C}_4\text{mim}][\text{NTf}_2]$ , (c)  $[\text{C}_6\text{mim}][\text{FAP}]$ , (d)  $[\text{C}_4\text{mpyr}][\text{NTf}_2]$ , (e)  $[\text{C}_4\text{mim}][\text{BF}_4]$ , (f)  $[\text{C}_4\text{mim}][\text{PF}_6]$ , (g)  $[\text{P}_{14,6,6,6}][\text{NTf}_2]$  and (h)  $[\text{P}_{14,6,6,6}][\text{FAP}]$ . Dot dashed line is the first scan, solid line is the second scan and dotted line is the response in the absence of oxygen.

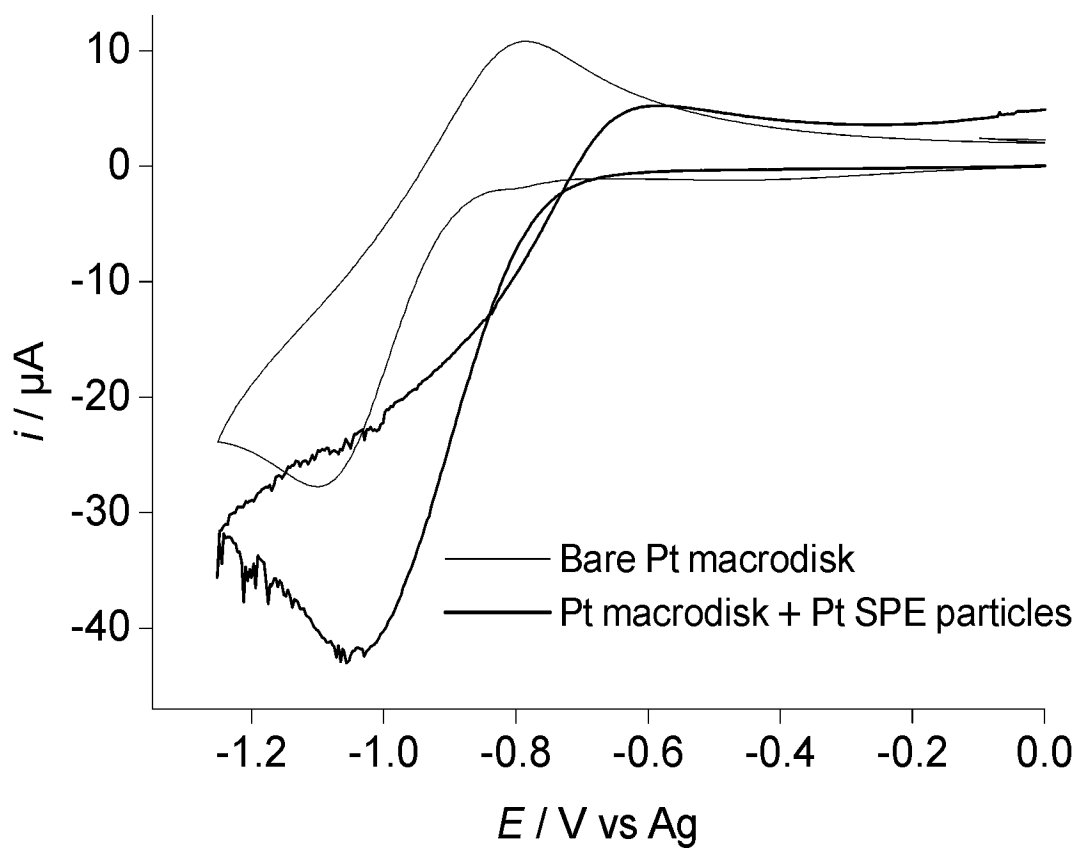


**Figure 5.** Cyclic voltammetry for 100 %  $\text{O}_2$  in  $[\text{C}_2\text{mim}][\text{NTf}_2]$  at a scan rate of  $100 \text{ mVs}^{-1}$ . Thin line=response on a bare Pt macrodisk electrode ( $d=1.6 \text{ mm}$ ) and thicker line= response on the same electrode covered with Pt SPE particles.

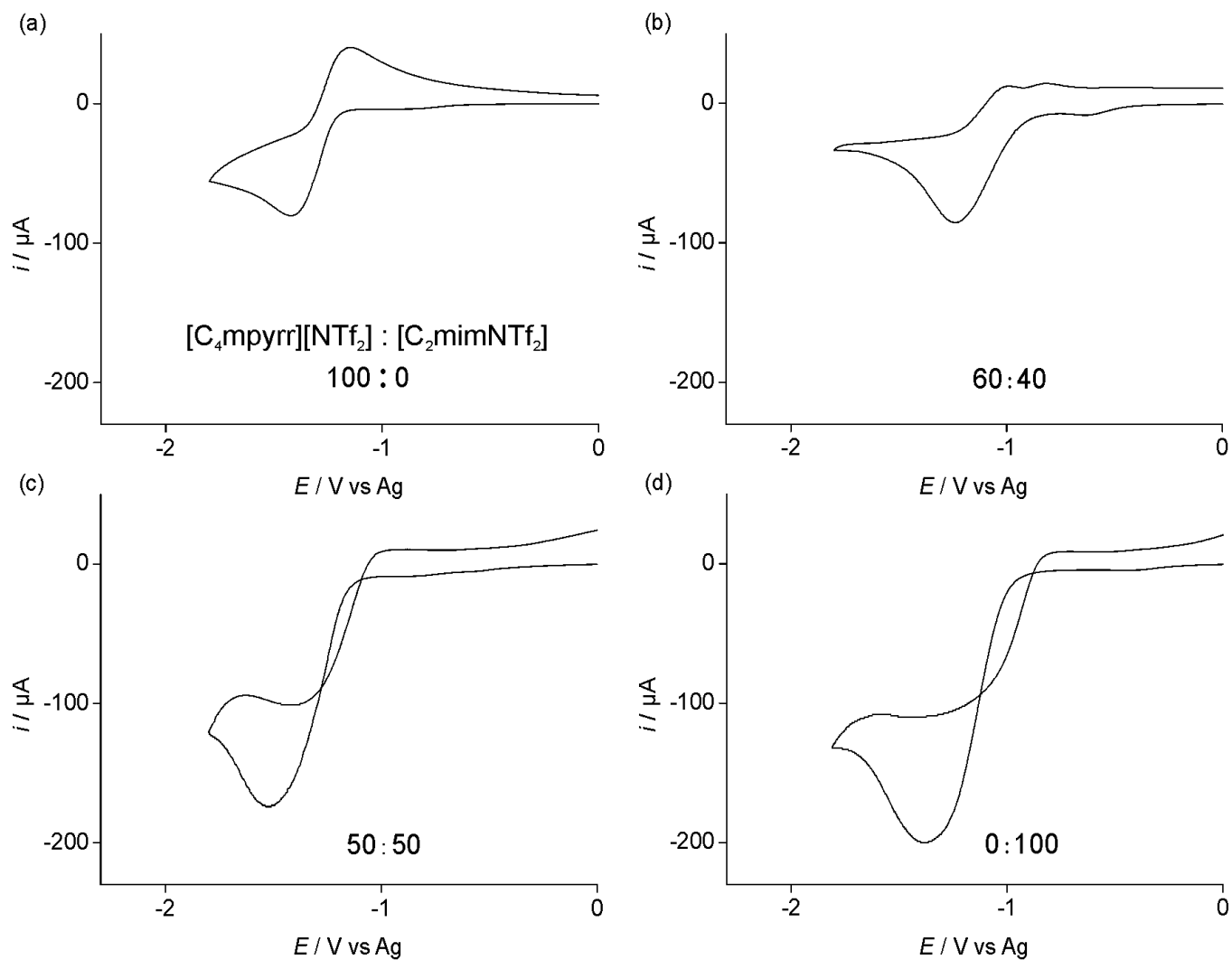
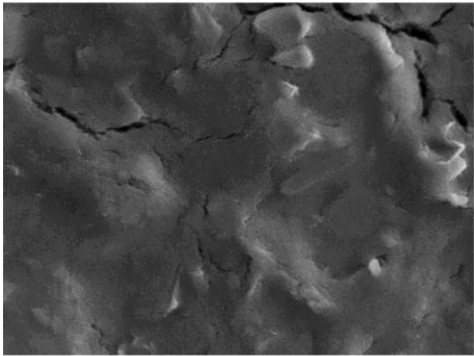
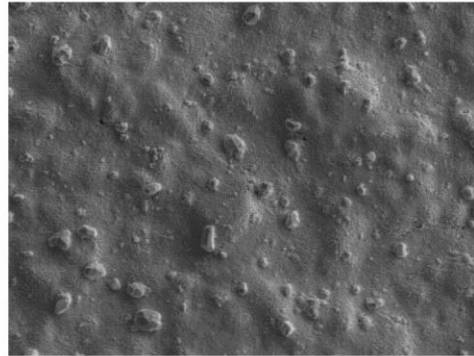


**Figure 6.** Cyclic voltammetry for 100 %  $\text{O}_2$  on a DropSens Pt electrode at a scan rate of  $100 \text{ mVs}^{-1}$  in electrolytes with different  $[\text{C}_4\text{mpyr}][\text{NTf}_2]:[\text{C}_2\text{mim}][\text{NTf}_2]$  mixing-ratios. (a) 100:0, (b) 60:40, (c) 50:50 and (d) 0:100.

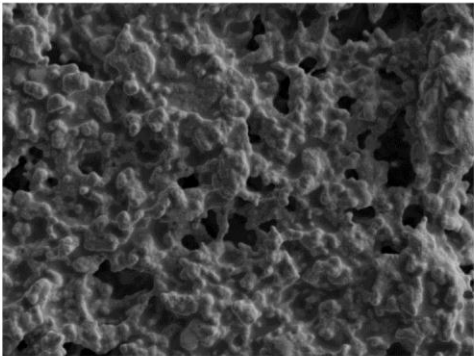
a) Carbon



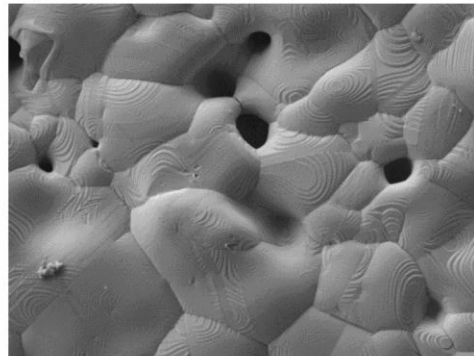
b) Gold



c) Platinum



d) Silver



┆ 4μm

**Figure 7.** Scanning electron micrographs of untreated DropSens working electrodes. (a) Carbon, (b) gold, (c) platinum and (d) silver screen-printed electrodes

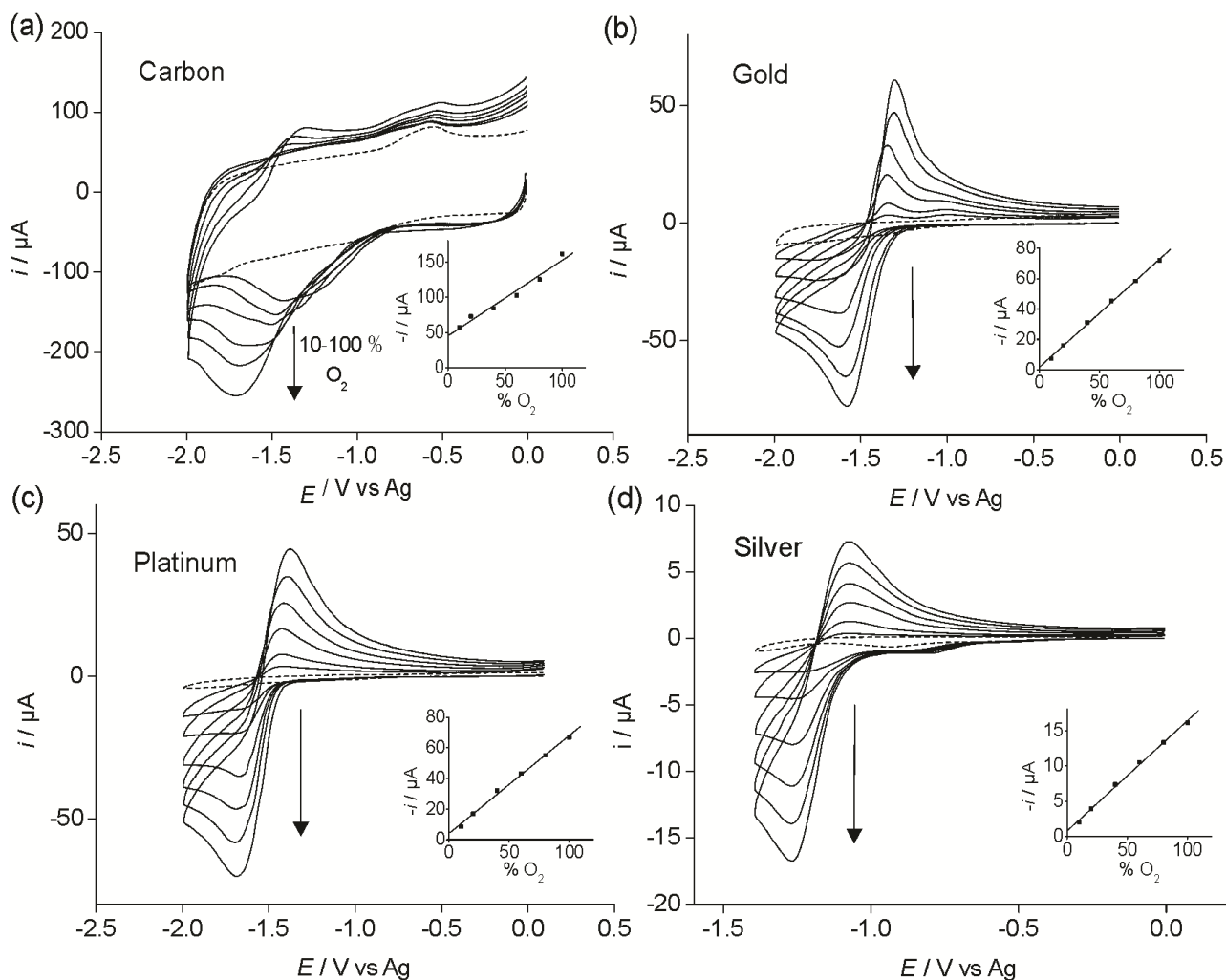


**Figure 8.** Cyclic voltammetry for  $O_2$  reduction in  $[C_4\text{mpyrr}][\text{NTf}_2]$  on (a) C, (b) Au, (c) Pt and (d) Ag SPEs at 10, 20, 40, 60, 80 and 100 vol %  $O_2$  at a scan rate of  $100 \text{ mVs}^{-1}$ . The dotted line is the response in the absence of oxygen. The insets are the corresponding plots of reduction peak current vs vol %  $O_2$  and the line of best-fit.

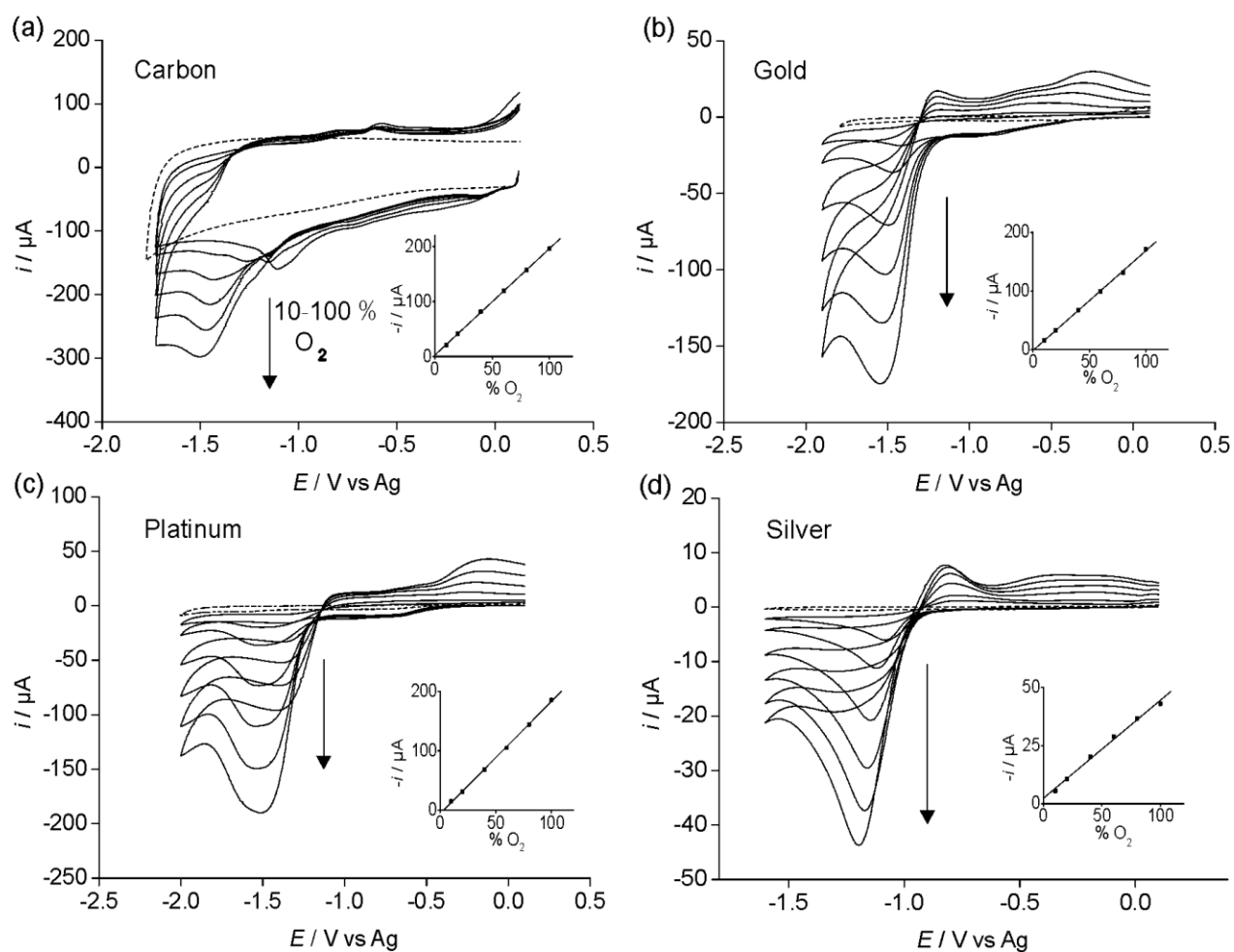


**Figure 9.** Cyclic voltammetry for  $O_2$  reduction in  $[C_2mim][NTf_2]$  on (a) C, (b) Au, (c) Pt and (d) Ag SPEs at 10, 20, 40, 60, 80 and 100 vol %  $O_2$  at a scan rate of  $100 \text{ mVs}^{-1}$ . The dotted line is the response in the absence of oxygen. The insets are the corresponding plots of reduction peak current vs vol %  $O_2$  and the line of best-fit.